JMR Noise Diode Stability and Recalibration Methodology after Three Years On-Orbit

Shannon Brown[1], Shailen Desai[1], Stephen Keihm[1], and Christopher Ruf[2]
[1]Jet Propulsion Laboratory, [2]University of Michigan
28 February 2006

1. Introduction

The Jason Microwave Radiometer (JMR) is included on the Jason-1 ocean altimetry satellite to measure the wet tropospheric path delay (PD) experienced by the radar altimeter signal. JMR is nadir pointing and measures the radiometric brightness temperature (T_B) at 18.7, 23.8 and 34.0 GHz. JMR is a Dicke radiometer and it is the first radiometer to be flown in space that uses noise diodes for calibration. Therefore, monitoring the long term stability of the noise diodes is essential. Each channel has three redundant noise diodes which are individually coupled into the antenna signal to provide an estimate of the gain.

Two significant jumps in the JMR path delays, relative to ground truth, were observed around 300 and 700 days into the mission. Slow drifts in the retrieved products were also evident over the entire mission. During a recalibration effort, it was determined that a single set of calibration coefficients was not able to remove the calibration jumps and drifts, suggesting that there was a change in the hardware and time dependent coefficients would be required. To facilitate the derivation of time dependent coefficients, an optimal estimation based calibration system was developed which iteratively determines that set of calibration coefficients which minimize the RMS difference between the JMR T_Bs and on-Earth hot and cold absolute references. This optimal calibration algorithm was used to fine tune the front end path loss coefficients and derive a time series of the JMR noise diode brightness temperatures for each of the nine diodes. Jumps and drifts, on the order of 1% to 2%, are observed among the noise diodes in the first three years on-orbit.

2. JMR Calibration Equations

The conversion of counts to T_B occurs in two processing steps for JMR. The first algorithm converts the raw counts to antenna temperatures, where the gain and offset are estimated using the noise diode and internal reference load. The second level of processing converts the antenna temperatures to main beam brightness temperatures using an antenna pattern correction algorithm. A simplified block diagram of a JMR radiometer chain is shown in Figure 1.

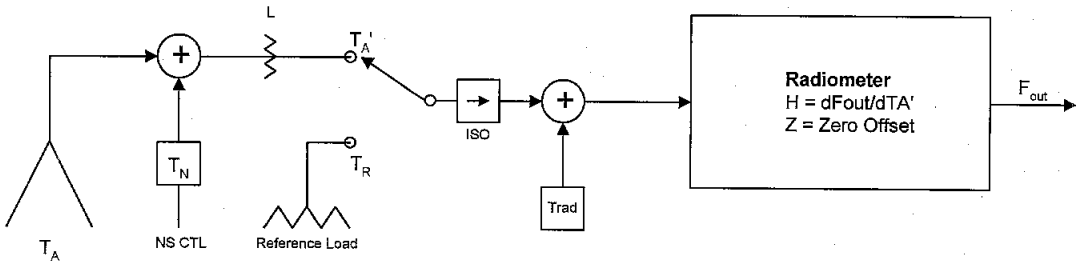

Figure 1. JMR simplified block diagram

Because the reference load is internal to the radiometer, the front end path loss before the Dicke switch must be accounted for in the antenna temperature calibration algorithm. The parameterized T_A equation is

$$T_A = \frac{C_A - C_R}{C_{N+A} - C_A} T_{ND} + K_R T_{\mathrm{Ref}} + K_{FH} T_{FH} \tag{1}$$

where C_A are the counts with the Dicke switch in the antenna position, C_R are the counts with the switch in the reference position, C_{N+A} are the counts in the antenna position with the noise diode switched on, T_{ND} is the effective noise diode brightness temperature, T_{Ref} is the physical temperature of the reference load, T_{FH} is the physical temperature of the feed horn and K_R and K_{FH} are front-end path loss coefficients. T_{ND} is expressed as a quadratic function of its physical temperature (T_{NS}) referenced to a nominal value, T_0,

$$T_{ND} = T_{NA} + T_{NB}(T_{NS} - T_0) + T_{NC}(T_{NS} - T_0)^2 \tag{2}$$

where T_{NA}, T_{NB} and T_{NC} are the coefficients. The calibration coefficients in Eons. (1) and (2) are estimated during pre-launch thermal-vacuum testing, but generally require fine tuning on-orbit. A dedicated post-launch calibration campaign was conducted during the first six months of the mission, at which time the calibration coefficients were adjusted to align the JMR T_Bs to on-Earth references. It was shown that the JMR path delay accuracy at this time exceeded the mission requirement of 1.2 cm RMS (Brown et al., 2004).

3. JMR Long Term Monitoring

Long term monitoring, subsequent to the post-launch calibration phase, indicated two shifts in the JMR PD retrieval of 0.5 cm and 1.5 cm, relative to various sources of ground truth, 300 days and 700 days into the mission. Ten day globally averaged JMR PDs compared to co-located ECMWF, SSM/I, TMI and GPS PD measurements are shown in Figure 2 for the first three years of the mission (a cycle is ~10 days).

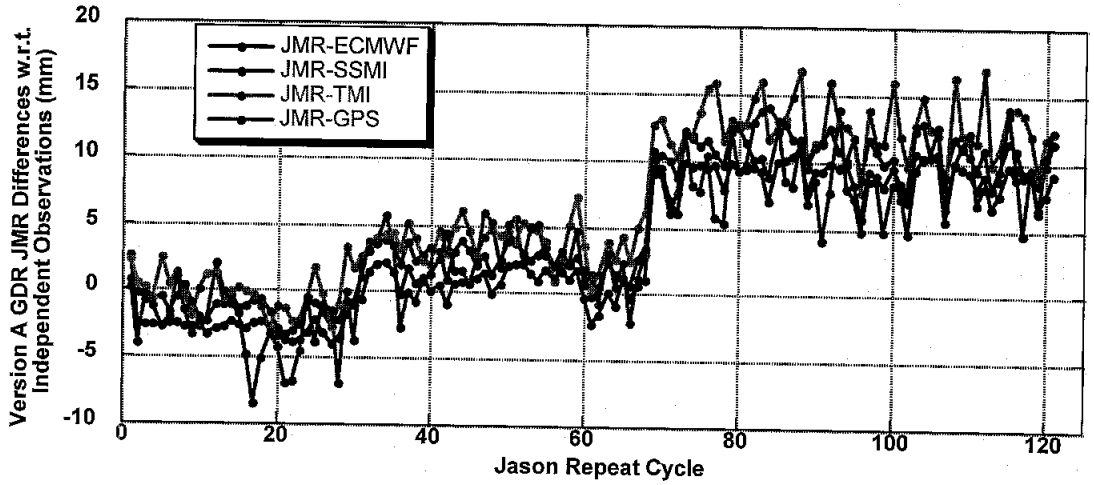

Figure 2. 10-day global averaged JMR path delay compared to various sources of ground truth.

An intermediate product of the PD algorithm is an estimate of the near-surface wind speed over the ocean. This estimate, differenced from the altimeter's estimate, is shown in Figure 3. A monotonic drift is evident over the course of the mission (note, the altimeter shows no drift compared to ECMWF). It is evident from these comparisons that there are two features in calibration which much be addressed, jumps and drifts. It is likely that a change in the 23.8 GHz channel calibration is responsible for the jumps and a change in the 34.0 GHz channel is responsible for the drift. This postulation is based on the weighting of each in the PD and WS algorithms, respectively.

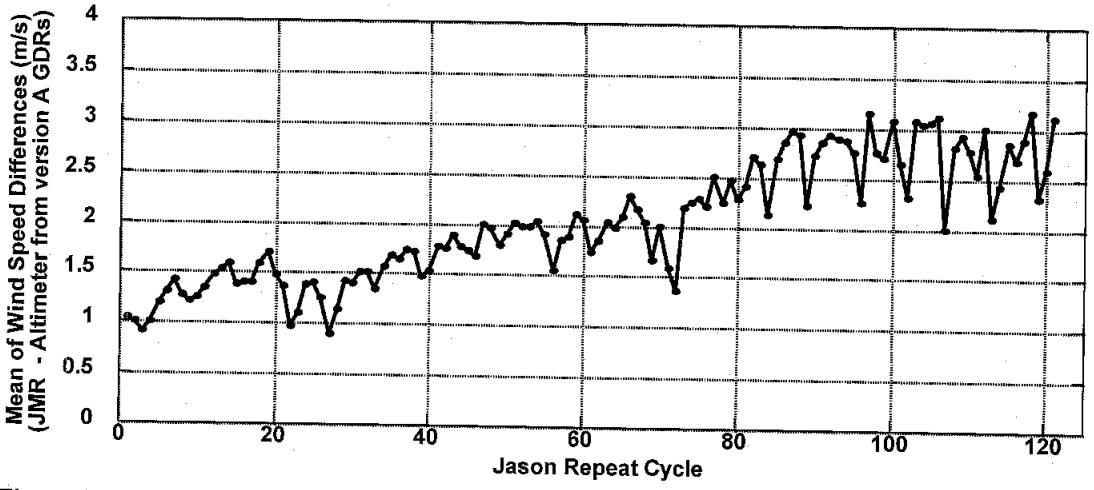

Figure 3. JMR – Altimeter wind speed retrievals for first three years of mission.

4. JMR Recalibration – Optimal Estimation

It is apparent from the PD and WS comparisons that a series of time dependent calibration coefficients is required to recalibrate the JMR. To facilitate this, an optimal estimation based calibration system is developed to find that set of calibration coefficients which minimize the RMS difference between the JMR T_{BS} and on-Earth hot and cold absolute T_B references. This technique employs, in an optimal way, the same

methodology used during the initial on-orbit cal/val. The optimal estimator is used (Rodgers, 2000)

$$\vec{x}^{(k+1)} = \vec{x}^{(k)} - \left[S_a^{-1} + J^T S_\varepsilon^{-1} J\right]^{-1}\left[J^T S_\varepsilon^{-1}\left(\vec{y} - F(\vec{x}^{(k)})\right) - S_a^{-1}\left(\vec{x}^{(k)} - \vec{x}_a\right)\right] \quad (3)$$

where $\vec{x}$ is a vector of calibration coefficients to be tuned, $\vec{x}_a$ is the *a priori* vector of calibration coefficients (i.e. pre-launch values), $\vec{y}$ is a vector of on-Earth T_B references, S_ε is the error covariance matrix for the T_B references and S_a is the error covariance matrix for the *a priori* coefficients. $F(\vec{x}^{(k)})$ is the forward model, representing the calibration algorithms which convert the raw counts to brightness temperatures using the k^{th} realization of the calibration coefficients. In eqn (3), the forward model also includes the algorithms which process the data for comparison to the on-Earth references (i.e. filtering, averaging, ect.). J is the Jacobian of the forward model, which is calculated numerically.

The *a priori* calibration coefficients can be taken initially as the pre-launch values. When generating time dependent coefficients, it is reasonable to set the *a priori* value to the most recent set, that is, the calibration coefficients determined for the time period previous to the current one. The *a priori* covariance matrix is also determined pre-launch and is an important component of the coefficient retrieval. This matrix determines the relative confidence among the coefficients. So in the case where two coefficients have a similar response on the calibration, the algorithm will preferentially adjust that which one has a lower confidence in.

At minimum, the T_B reference vector should include a hot reference and a cold reference to constrain the gain and offset terms in the calibration algorithms. A vicarious cold reference (Ruf, 2000) is used to anchor the T_Bs at the coldest end of the spectrum and pseudo-blackbody regions in the Amazon rainforest are used to calibrate the hottest T_Bs (Brown and Ruf, 2005). These references are equivalent to those used during the initial post-launch cal/val.

The optimal estimator drives the calibration to a hot and cold reference T_B, so it may seem that only two coefficients can be independently estimated, when in fact, several coefficients can be simultaneously estimated. Because the instrument temperature of the various components vary over an orbit and over the various beta angles of the satellite, the hot and cold references sampled over the many instrument temperature states are independent and therefore allow for an over-constrained estimate of the front-end path loss coefficients and noise diode brightness. This is also true of the other processing algorithms not addressed here. For example, coefficients in the antenna pattern correction algorithm, specifically those that correct for the on-Earth sidelobe contamination, can be tuned by sampling a T_B reference as a function of the measurement proximity to land.

5. Relative JMR ND Behavior

The relative JMR ND behavior is observed by bootstrapping the calibration from diode *i* to diode *j* and taking the difference from the value given by eqn. (2),

$$\Delta T_{ND}^{j} = \frac{C_{ND+A}^{j} - C_{A}^{j}}{C_{ND+A}^{i} - C_{A}^{i}} T_{ND0}^{i}(T_{NS}) - T_{ND0}^{j}(T_{NS}) \quad . \tag{4}$$

If the diodes are perfectly stable, then ΔT_{ND}^{j} will be a constant. If either diode i or j change, then ΔT_{ND}^{j} will vary. Equation (4) is useful only for determining relative changes among the diodes. An independent reference is required to determine the absolute magnitude of any changes observed between the diodes. Figure 4 shows the value of eqn. (4) for the 6 possible combinations among the 3 diodes for each channel at T_{NS} = 287.7 $\pm$ 0.1 K. It is evident from these plots that there exist non-thermal changes, on the order of 1-2% in T_{ND}, over the first three years of the mission. The effective brightness of the diodes is between 90-200 K.

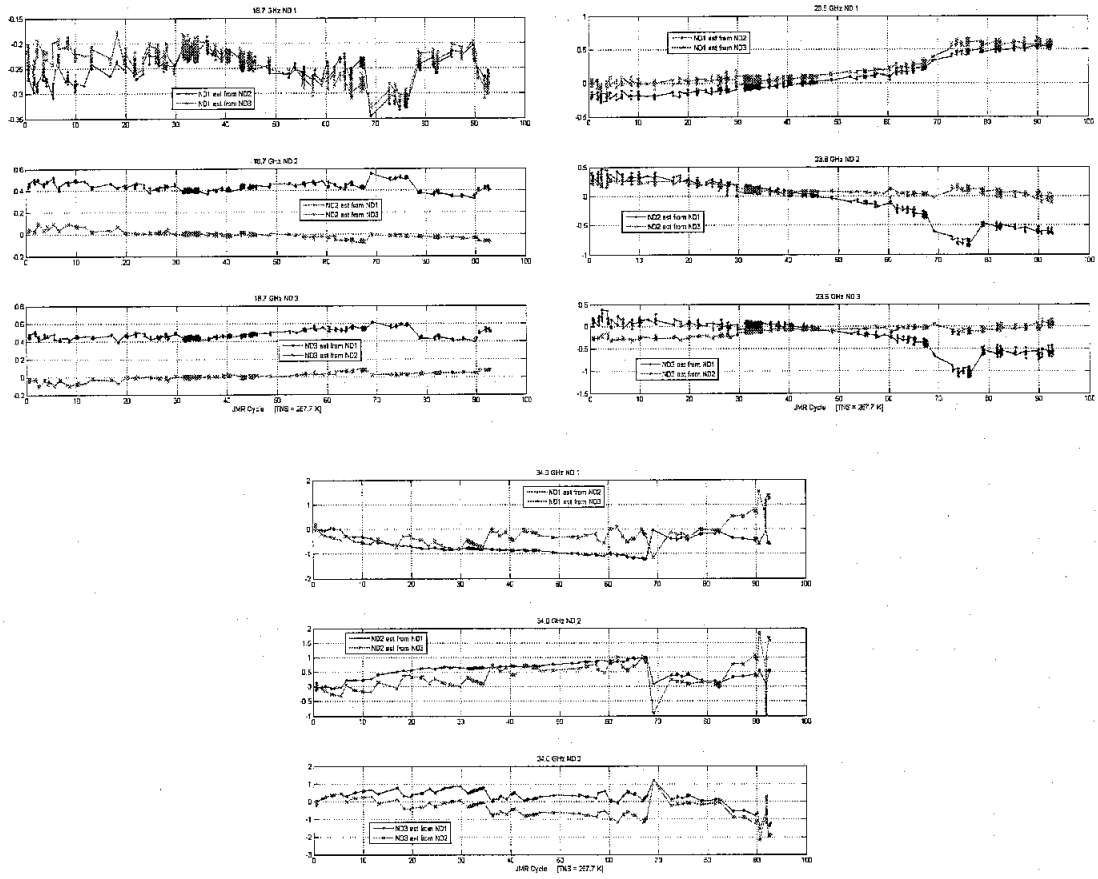

Figure 4. Bootstrapping the ND calibration for the different combinations between the three noise diodes (18.7 GHz upper left, 23.8 GHz upper right, 34.0 GHz lower). These plots are for a physical noise diode temperature of 287.7 $\pm$ 0.1 K.

6. Derived JMR T_{NA} Time Series

The JMR optimal estimation software is used to estimate a time series of JMR noise diode brightness, T_{NA} in eqn. (2) . The front end loss coefficients are assumed constant with time and are set equal to those derived from the first 300 days of the mission using the calibration software. The linear and quadratic coefficients in eqn. (2) have not been tuned on orbit and may have some error associated with them. To minimize the possibility of errors in the temperature dependent T_{ND} correction showing up in the time series as drifts or offsets, only noise source temperatures between 287 and 288 K were considered. The reference value, T_0, in eqn (2) is 287.5 K. The full dynamic range of T_{NS} on-orbit is 285 – 298 K. The linear temperature coefficient is low for the diodes, near 0.02 K/K for the 18.7 and 23.8 GHz diodes and approximately 0.2 K/K for the 34.0 GHz diodes.

The optimization software is used to estimate T_{NA} for 15 day blocks of JMR data with the references sampled every three days. This essentially gives a running average of the noise diode brightness with a 15 day averaging window. Figure 5 shows the T_{NA} time series estimated for the JMR noise diodes. These figures clearly show jumps in the 23.8 GHz noise diodes at cycle 30 and cycle 69, which correspond to the observed jumps in PD. Drifts in the 18.7 and 34.0 GHz channels are also clearly visible. Inter-jump drifts are evident in the 23.8 GHz channel. A smoothed line is included with the data. Only one diode appears to be stable over the first three years and that is the 34.0 GHz ND2.

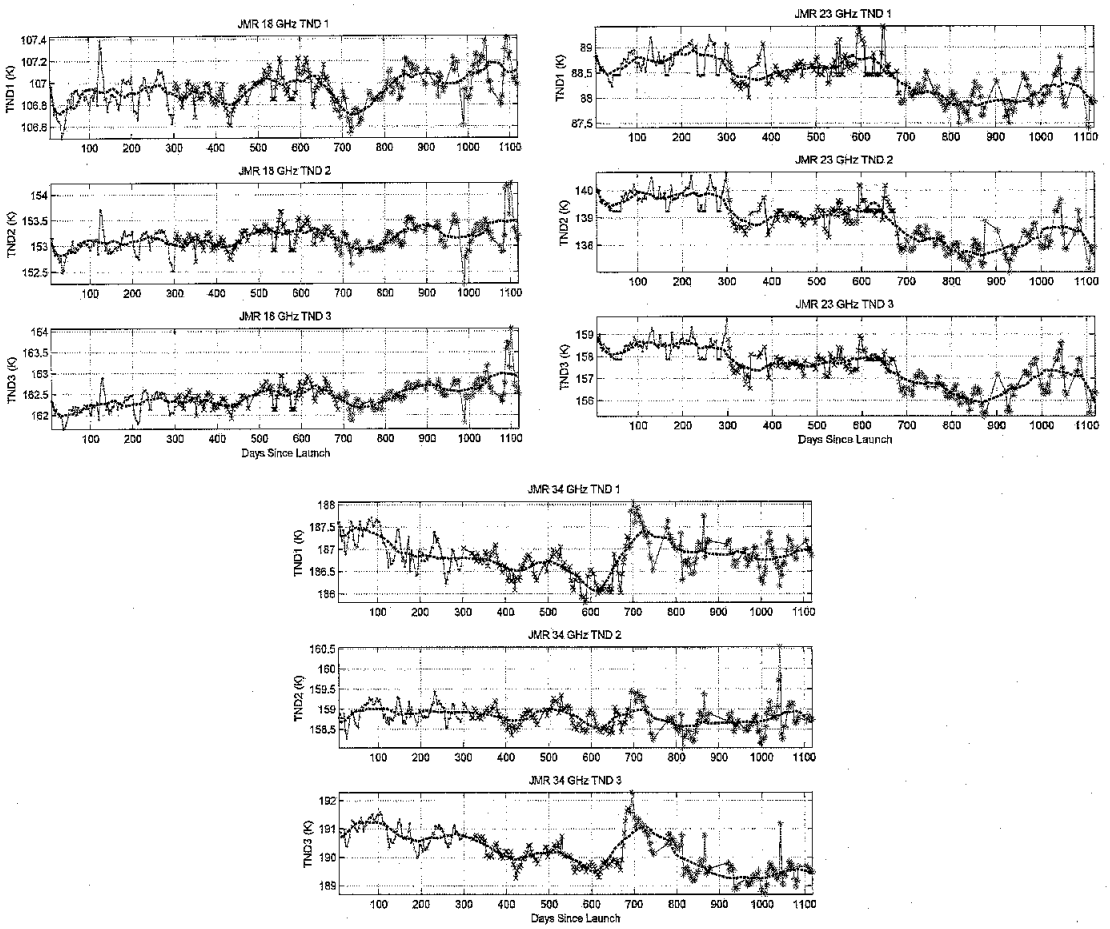

Figure 5. JMR 18.7 (top left), 23.8 (top right) and 34.0 (bottom) GHz T_{NA} versus day of year for 287 < T_{NS} < 288. T_0 is equal to 287.5.

7. Retrieved T_{ND} Validation

The validity of the retrieved T_{ND} time series is first assessed by observing recalibrated PD comparisons. The discrete jumps should be eliminated with the updated calibration, and this is indeed the case, as is shown in Figure 6. The T_{ND} time series should also eliminate the relative drifts between the diodes shown in Figure 4. Figure 7 shows ΔT_{ND}^{j} with the T_{ND} time series used in placed of the static coefficient. It can be seen that the retrieved time series does eliminate the relative changes among the diodes. This validates the assumption that the noise diode brightness is the only hardware change in the system. Because the noise diode brightness was retrieved solely and independently by forcing the T_Bs to agree with the on-Earth references, a change in another system constant would be introduced into the noise diode time series in error. That is, the relative behavior between the diodes would not be conserved in this case.

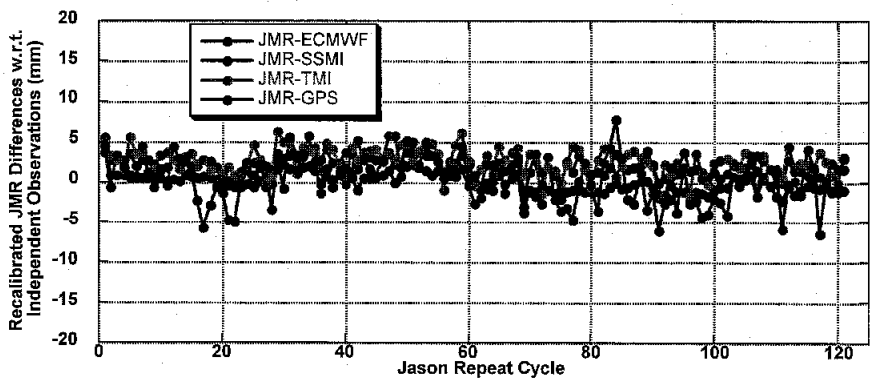

Figure 6. JMR recalibrated PDs compared to various other PD estimates.

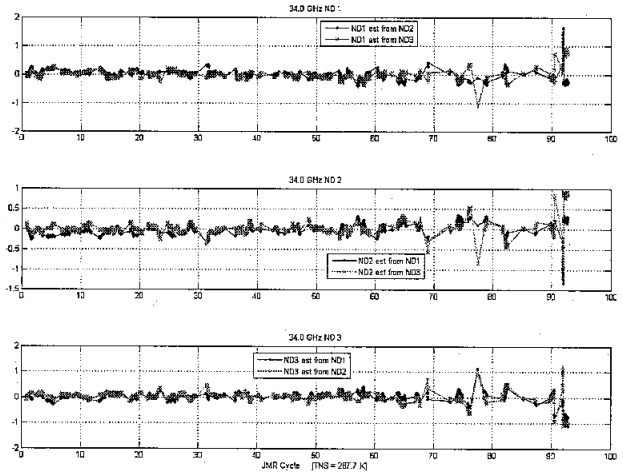

Figure 7. Bootstrapping the 34.0 GHz ND calibration for the different combinations between the three noise diodes. These plots are for a physical noise diode temperature of 287.7 + 0.1 K. The retrieved ND time series is used for this plot.

8. Conclusions

JMR is the first radiometer to be flown in space that uses noise diodes for calibration. Therefore the long term monitoring of this radiometer's calibration is essential. Changes in the JMR geophysical retrievals relative to ground truth were observed during the first three years of the mission. An optimal estimation based calibration system is developed to estimate that set of calibration coefficients which minimize the RMS difference between the JMR T_Bs and on-Earth hot and cold references. The changes in the JMR calibration were linked to changes in the JMR ND brightness based on the observation of their output relative to each other. The calibration system is used to derive a time series of the JMR ND effective brightness temperature. Drifts and jumps, on the order of 1-2%, were observed in the retrieved time series. It is shown that these time variable coefficients remove the jumps in the PD retrievals and eliminate the relative changes between the diodes.

References

Rodgers, C. 2000. Inverse Methods for Atmospheric Sounding: Theory and Practice. World Scientific Publishing Co. River Edge, NJ. 83-85

Brown, S., C. Ruf, S. Keihm and A. Kitiyakara, "Jason Microwave radiometer performance and on-orbit calibration", Marine Geodesy, no. 27, vol. 1, Jan-June 2004, pg 199-220.

Brown, S. and C. Ruf. 2005. Determination of an Amazon Hot Reference Target for the On-Orbit Calibration of Microwave Radiometers. *J. Atm. Ocean. Sci.* 22. pp 1340-1352.

Ruf, C. 2000. Detection of Calibration Drifts in Spaceborne Microwave Radiometers Using a Vicarious Cold Reference. *IEEE Trans. Geosci. Rem. Sens.* vol 38. pp. 44-52.